Comparison of the Susceptibility to Implant Failure in the Lateral, Posterior, and Transforaminal Lumbar Interbody Fusion: A Finite Element Analysis

Ryo Oikawa[1], Hideki Murakami[1], Hirooki Endo[1], Hirotaka Yan[1], Daisuke Yamabe[1], Yusuke Chiba[1], Ryosuke Oikawa[1], Norihiro Nishida[2], Xian Chen[3], Takashi Sakai[2], Minoru Doita[1]

■ OBJECTIVE: **There are several techniques for lumbar interbody fusion, and implant failure following lumbar interbody fusion can be troublesome. This study aimed to compare the stress in posterior implant and peri-screw vertebral bodies among lateral lumbar interbody fusion (LLIF), posterior lumbar interbody fusion (PLIF), and transforaminal lumbar interbody fusion (TLIF) and to select the technique that is least likely to cause implant failure.**

■ METHODS: **We created an intact L3–L5 model and simulated the LLIF, PLIF, and TLIF techniques at L4–L5 using finite element methods. All models at the lower portion of L5 were fixed and imposed a preload of 400 N and a moment of 7.5 Nm on the upper portion of L3 to simulate flexion, extension, lateral bending, and axial rotation. We investigated the peak stresses and stress concentration in the posterior implant and peri-screw vertebral bodies for the LLIF, PLIF, and TLIF techniques.**

■ RESULTS: **The extension, flexion, bending, and rotation peak stresses and stress concentration in the posterior implant, as well as the peri-screw vertebral bodies, were the lowest in LLIF, followed by PLIF and TLIF.**

■ CONCLUSIONS: **It was found that implant failure was least likely to occur in LLIF, followed by PLIF and TLIF. Hence, surgeons should be aware of these factors when selecting an appropriate surgical technique and be careful for implant failure during postoperative follow-up.**

INTRODUCTION

Low back pain (LBP) is one of the most prevalent complaints in the world (prevalence: 9.17%),[1] and many elderly people with lumbar spinal canal stenosis (LSCS) suffer from LBP. Conservative treatment is the first choice for LBP caused by LSCS. However, if people have neurologic leg pain associated with LBP, it is often difficult to treat and resist conservative treatment.[2] In such cases, surgery may be performed. In lumbar spondylolisthesis, there is an unfirm displacement of the lumbar vertebrae, which causes LSCS and compression or stretching of nerves, leading to neurologic leg pain. Hence, the surgical treatment for lumbar spondylolisthesis involves decompression, lumbar interbody fusion, and spinal fusion with the pedicle screw. Since the inception of lumbar interbody fusion, 2 major posterior approaches, such as the posterior lumbar interbody

Key words
- Finite element analysis
- Implant failure
- Implant fracture
- Lateral lumbar interbody fusion
- Posterior lumbar interbody fusion
- Screw loosening
- Transforaminal lumbar interbody fusion

Abbreviations and Acronyms
CL: Capsular ligament
CT: Computed tomography
FE: Finite element
ISL: Interspinous ligament
IVD: Intervertebral disc
LBP: Low back pain
LF: Ligamentum flavum
LLIF: Lateral lumbar interbody fusion
LSCS: Lumbar spinal canal stenosis
PLIF: Posterior lumbar interbody fusion
PLL: Posterior longitudinal ligament
ROM: Range of motion
SSL: Supraspinous ligament
TLIF: Transforaminal lumbar interbody fusion

From the [1]Department of Orthopedic Surgery, Iwate Medical University, Yahaba Town, Iwate Prefecture; [2]Department of Orthopedic Surgery, Yamaguchi University Graduate School of Medicine, Ube City, Yamaguchi Prefecture; and [3]Faculty of Engineering, Yamaguchi University, Ube City, Yamaguchi Prefecture, Japan

To whom correspondence should be addressed: Hideki Murakami, M.D., Ph.D. [E-mail: hmura@iwate-med.ac.jp]

Citation: World Neurosurg. (2022) 164:e835-e843.
https://doi.org/10.1016/j.wneu.2022.05.056

*Journal homepage: **www.journals.elsevier.com/world-neurosurgery***

*Available online: **www.sciencedirect.com***

fusion (PLIF) and transforaminal lumbar interbody fusion (TLIF), have been widely performed. Furthermore, in recent years, lateral lumbar interbody fusion (LLIF) has been performed frequently since it allows the insertion of larger cages and indirect decompression with a minimally invasive technique.[3] Although there are several techniques for lumbar interbody fusion, implant failures, such as implant fracture and screw loosening following lumbar interbody fusion, could be troublesome.

Previous studies have compared the stresses of posterior implants in PLIF and TLIF,[4] as well as in the anterior lumbar interbody fusion, PLIF, and TLIF,[5] using the finite element (FE) method. However, the stresses in the posterior implant in LLIF, PLIF, and TLIF have not yet been investigated. Furthermore, increased stress on the vertebral body causes trabecular bone injury.[6] Nevertheless, the stresses on the peri-screw vertebral bodies in LLIF, PLIF, and TLIF have not been investigated yet. We hypothesized that the effects on the stresses in the posterior implant and peri-screw vertebral bodies would change when comparing LLIF, PLIF, and TLIF.

The study aims to compare the 3 techniques of LLIF, PLIF, and TLIF. This is to confirm the stresses of the posterior implant and peri-screw vertebral bodies using the FE method and to identify a better technique that is less likely to cause implant failure after lumbar interbody fusion.

MATERIALS AND METHODS

FE Model of the Intact Lumbar Vertebrae

This study was approved by the institutional review board (H28-054 and MH2021-042). A 3-dimensional FE model, which consisted of the L3–L5 vertebrae, anterior longitudinal ligament, posterior longitudinal ligament (PLL), ligamentum flavum (LF), and intervertebral disc (IVD), was created using computed tomography (CT) images of an adult woman. The vertebral body was divided into cortical and

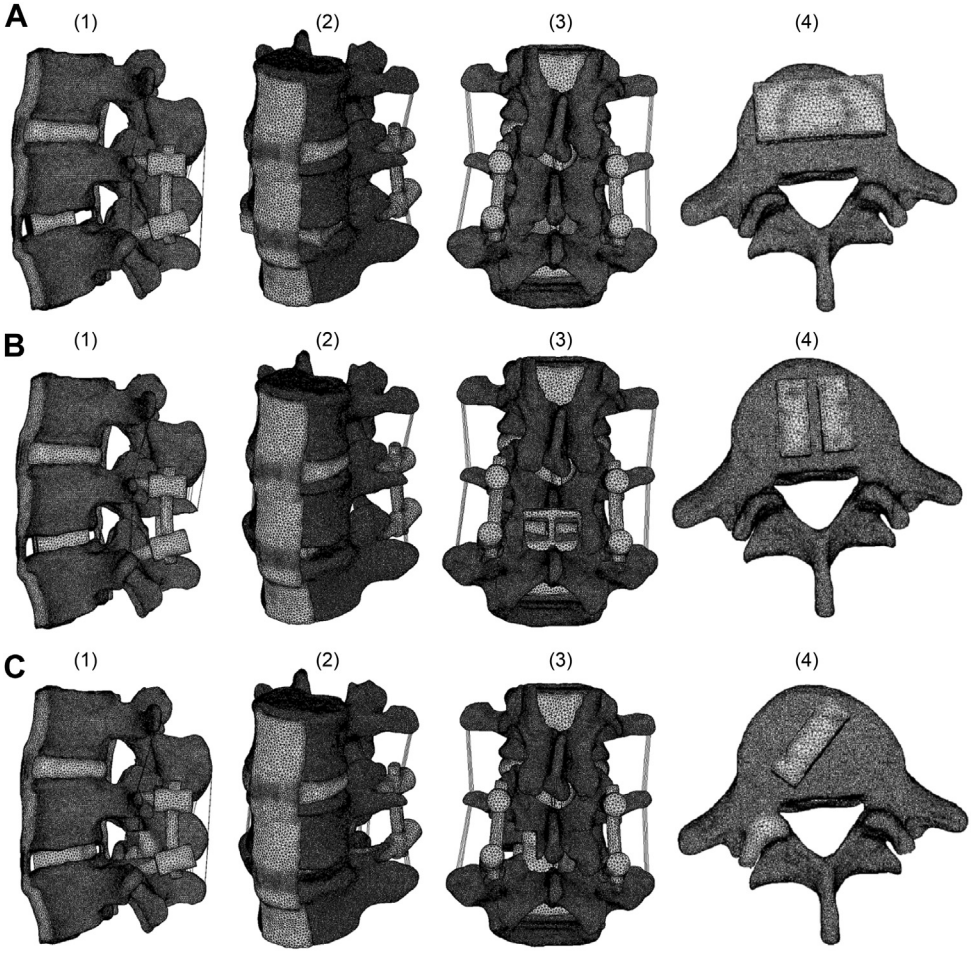

Figure 1. Models of lumbar interbody fusion. (**A**) Lateral lumbar interbody fusion. (**B**) Posterior lumbar interbody fusion. (**C**) Transforaminal lumbar interbody fusion. (1) Lateral, (2) oblique, and (3) posterior views of the models and (4) the location of the interbody cage.

Table 1. Material Properties of the Present Model

	Young Modulus (MPa)	Poisson Ratio	Cross-Sectional Area (mm^2)
Cortical bone	12,000	0.3	
Cancellous bone	100	0.3	
Annulus fibrosus	4.2	0.45	
Nucleus pulposus	1	0.49	
Anterior longitudinal ligament	20	0.3	
Posterior longitudinal ligament	20	0.3	
Ligamentum flavum	19.5	0.3	
Interspinous ligament	11.6	0.3	40
Supraspinous ligament	15	0.3	30
Intertransverse ligament	58.7	0.3	3.6
Capsular ligament	32.9	0.3	60
Cage (PEEK)	3500	0.3	
Pedicle screw (titanium alloy)	113,000	0.3	
Rod (titanium alloy)	113,000	0.3	

PEEK, polyetheretherketone.

cancellous bones based on the actual CT measurements to allow a cortical shell thickness ranging from 1.5 to 2.0 mm, and the IVD was divided into the annulus fibrosus and nucleus pulposus. We used the Simpleware ScanIP, Version R-2020.9 (Synopsys, Inc., Mountain View, CA, USA). Additionally, the truss element simulated the posterior ligaments (capsular ligament, CL; interspinous ligament, ISL; supraspinous ligament, SSL; intertransverse ligament). Each ligament type had a distinct cross-sectional area. In each segment, 16, 3, 2, and 8 truss elements were used to simulate the CL, ISL, SSL, and intertransverse ligament, respectively.[7] We used the Patran 2019 FP1 SP1 (MSC Software, Inc., Newport Beach, CA, USA) to make these truss elements.

FE Model of Posterior Implant and LIF Procedure

The intact L3–L5 model was modified to simulate LLIF, PLIF, and TLIF at the L4–L5 level, respectively, with 4 pedicle screws (diameter = 6.5 mm and length = 45 mm) and 2 rods (diameter = 5.5 mm). These were optimally fabricated using the Simpleware ScanIP. The simulated surgical procedure for LLIF inserted a cuboid resembling an LLIF cage (height, 9 mm; length, 40 mm; and width, 18 mm) at the L4–L5 intervertebral space[8] which removed the entire IVD (Figure 1A). The simulated surgical procedure for PLIF removed partial lamina, bilateral medial facet joints, partial PLL, entire SSL, entire ISL, entire LF, and entire IVD at L4–L5 and inserted 2 cuboids resembling a PLIF cage (height, 9 mm; length, 22 mm; and width, 9 mm), which were placed in parallel at the L4–L5 intervertebral space based on previous literature[4] (Figure 1B). The simulated surgical procedure for TLIF removed the entire left facet joint (including the CL), left LF, and entire IVD at L4–L5 and inserted a cuboid resembling a TLIF cage (height, 9 mm; length, 22 mm; and width, 9 mm), which was placed obliquely at 45° at the L4–L5 intervertebral space based on previous literature[9] (Figure 1C).

Table 2. Validation of the Present Finite Element Model Against Previous Study

	Extension (°)	Flexion (°)	Lateral Bending (°)	Axial Rotation (°)
L3-L4				
Niosi et al.[20]	2.4 ± 0.9	4.4 ± 2.0	2.4 ± 1.2	1.2 ± 0.5
Schmoelz et al.[21]	5.0 ± 1.0	4.0 ± 1.3	4.7 ± 2.0	1.0 ± 0.6
Present study	2.03	4.14	4.10 (L)	1.16 (L)
			3.56 (R)	1.34 (R)
L4-L5				
Schilling et al.[22]	3.32 ± 1.12	5.62 ± 2.17	7.76 ± 1.85	5.16 ± 1.30
Shim et al.[23]	2.79 ± 0.42	5.48 ± 0.88	4.45 ± 1.01	3.80 ± 0.99
Yang et al.[24]	1.70	2.16	1.40 (L)	0.90 (L)
			1.84 (R)	0.96 (R)
Present study	3.23	4.25	5.01 (L)	1.01 (L)
			5.45 (R)	1.16 (R)

Material Properties and Boundary Conditions

All FE analyses were performed using the Patran. The bone-cage and bone-screw interfaces and screw-rod connections were assigned and bonded entirely by node sharing. A tetrahedral mesh was generated on the vertebra, IVD, anterior longitudinal ligament, PLL, and LF. After node sharing, the intact model had a total of 368,617 nodal points and 1,846,289 elements. The material properties of the anatomical parts were set based on previous studies,[10-14] and titanium alloy (Ti-6Al-4V) was selected as the material for the posterior implants (Table 1).[15,16] Polyetheretherketone was selected as the material for the interbody cages (Table 1).[16,17] All FE models at the lower L5 were fixed and imposed a preload of 400 N and a moment of 7.5 Nm on the superior L3 to simulate flexion, extension, lateral bending, and axial rotation.[4,9] We investigated the von Mises stress in the posterior implant and peri-screw vertebral bodies in the LLIF, PLIF, and TLIF.

RESULTS

Model Validation

The range of motion (ROM) of L3–L4 in extension, flexion, left bending, right bending, left rotation, and right rotation was 2.03°, 4.14°, 4.10°, 3.56°, 1.16°, and 1.34°, respectively (Table 2). The ROM of L4–L5 in extension, flexion, left bending, right

Table 3. The Peak von Mises Stress of the Pedicle Screw Fixation (Unit: MPa)

	LLIF*	PLIF†	TLIF‡
Extension			
L4 left screw	48.8	66.2	55.0
L4 right screw	49.7	52.9	48.7
L5 left screw	38.2	43.6	35.4
L5 right screw	37.5	40.2	46.7
Left rod	60.6	57.4	56.8
Right rod	55.1	59.9	71.2
Flexion			
L4 left screw	20.3	17.8	30.3
L4 right screw	18.2	24.2	21.1
L5 left screw	11.3	27.8	31.8
L5 right screw	14.3	28.8	32.0
Left rod	10.7	14.9	16.9
Right rod	9.35	23.1	41.0
Lt bending			
L4 left screw	25.3	28.4	34.2
L4 right screw	13.9	17.8	16.6
L5 left screw	11.7	22.6	26.7
L5 right screw	9.04	22.0	26.2
Left rod	26.4	40.0	45.0
Right rod	11.5	10.1	14.5
Rt bending			
L4 left screw	18.7	16.3	28.7
L4 right screw	16.2	30.8	44.1
L5 left screw	8.35	21.2	28.3
L5 right screw	13.3	34.1	52.8
Left rod	12.7	21.1	29.2
Right rod	24.0	56.7	83.6
Lt rotation			
L4 left screw	39.8	52.1	42.2
L4 right screw	25.1	26.0	26.3
L5 left screw	47.9	62.6	63.2
L5 right screw	39.3	41.7	45.1
Left rod	40.9	49.1	50.6
Right rod	36.2	32.2	30.0
Rt rotation			
L4 left screw	34.1	33.2	37.8
L4 right screw	41.9	52.8	62.4
L5 left screw	34.6	39.7	44.8
L5 right screw	46.6	65.9	80.7
Left rod	41.6	34.9	34.2
Right rod	36.2	52.2	61.5

*LLIF, lateral lumbar interbody fusion.
†PLIF, posterior lumbar interbody fusion.
‡TLIF, transforaminal lumbar interbody fusion.

Continues

bending, left rotation, and right rotation was 3.23°, 4.25°, 5.10°, 5.45°, 1.01°, and 1.16°, respectively (Table 2).

The von Mises Stresses of Posterior Implants

The von Mises stresses in the posterior implants of the LLIF, PLIF, and TLIF models are shown in Table 3. For the LLIF model, the following data of the peak von Mises stress were obtained: extension (60.6 MPa), flexion (20.3 MPa), left bending (26.4 MPa), right bending (24.0 MPa), left rotation (47.9 MPa), and right rotation (46.6 MPa). For the PLIF model, the following data of the peak von Mises stress were found: extension (66.2 MPa), flexion (28.8 MPa), left bending (40.0 MPa), right bending (56.7 MPa), left rotation (62.6 MPa), and right rotation (65.9 MPa). For the TLIF model, the following data of the peak von Mises stress were found: extension (71.2 MPa), flexion (41.0 MPa), left bending (45.0 MPa), right bending (83.6 MPa), left rotation (63.2 MPa), and right rotation (80.7 MPa). With this, the LLIF model had the lowest peak von Mises stresses, and the TLIF model was the highest among all directions (Figure 2). Additionally, the stress concentration was found to be the lowest and highest in the LLIF and TLIF, respectively (Figure 3).

The von Mises Stresses of Peri-Screw Vertebral Bodies

The von Mises stresses of the peri-screw vertebral bodies of the LLIF, PLIF, and TLIF models are shown in Table 4. For the LLIF model, the following data of the peak von Mises stresses were obtained: extension (66.5 MPa), flexion (17.6 MPa), left bending (10.7 MPa), right bending (12.1 MPa), left rotation (35.6 MPa), and right rotation (47.5 MPa). For the PLIF model, the following data of the peak von Mises stresses were found: extension (71.7 MPa), flexion (26.4 MPa), left bending (17.3 MPa), right bending (18.8 MPa), left rotation (50.1 MPa), and right rotation (51.5 MPa). For the TLIF model, the following data of the peak von Mises stresses were obtained: extension (78.0 MPa), flexion (30.6 MPa), left bending (21.8 MPa), right bending (21.1 MPa), left rotation (50.9 MPa), and right rotation (55.7 MPa). With this, the LLIF model had the lowest peak von Mises stresses, and the TLIF model was the highest among all directions (Figure 4). Additionally, the stress concentration was found to be the lowest and highest in the LLIF and TLIF, respectively (Figure 5).

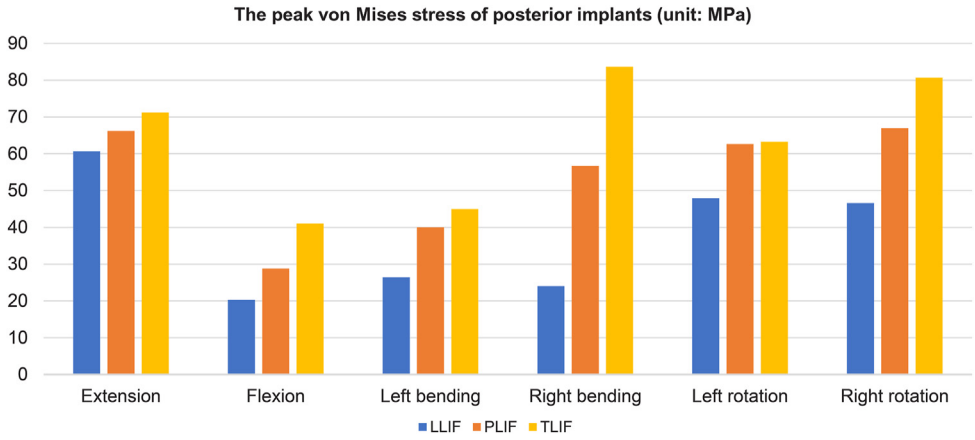

Figure 2. Comparison of the peak von Mises stress of posterior implants in the lateral lumbar interbody fusion (LLIF), posterior lumbar interbody fusion (PLIF), and transforaminal lumbar interbody fusion (TLIF).

DISCUSSION

The FE method is a computational method that uses computers to solve problems in structural mechanics, and it enables the analysis of complex structures.[18] In orthopedics, it was first used in 1972 to calculate stresses in bones.[19] Since then, many studies have used this method in the spine, wherein the structures of bones, joints, and ligaments are more complex. Based on these characteristics, we also conducted a biomechanical study using this method.

We compared the von Mises stresses of the posterior implants and peri-screw vertebral bodies using the FE method in LLIF, PLIF, and TLIF. This was to compare the risk of postoperative implant failures, such as implant fracture and screw loosening.

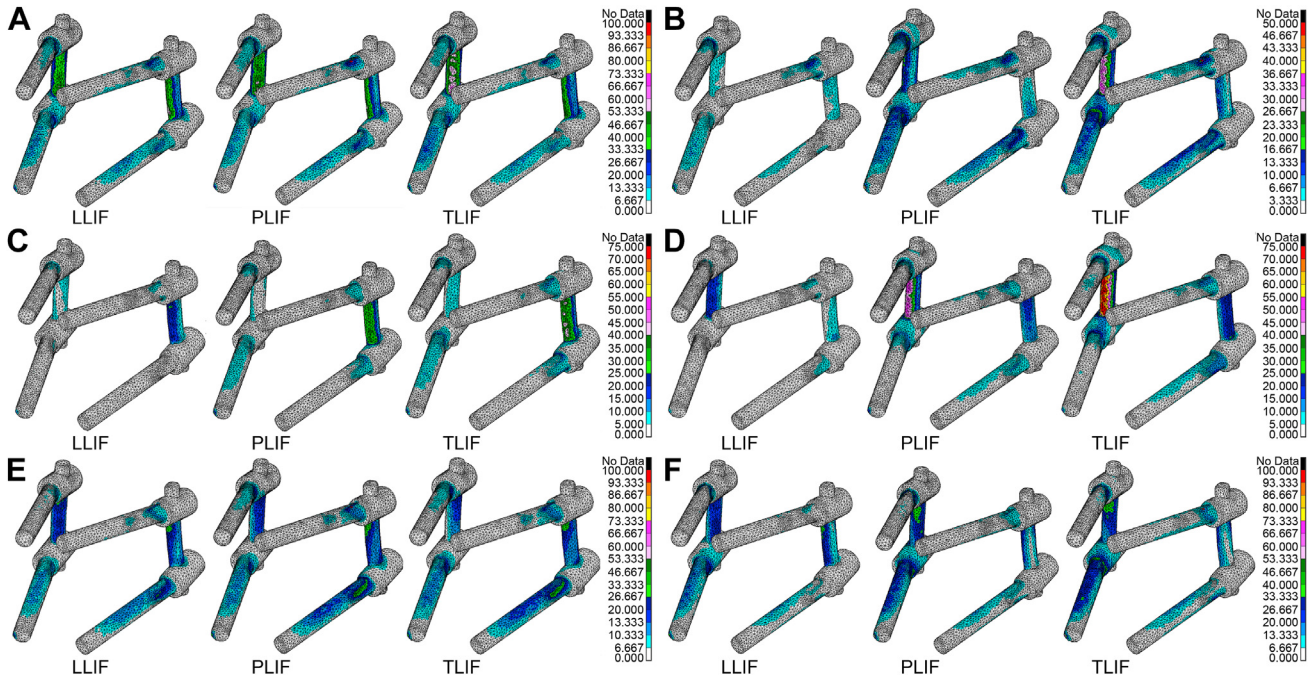

Figure 3. Stress concentration in the posterior implants. (**A**) Extension, (**B**) flexion, (**C**) left bending, (**D**) right bending, (**E**) left rotation, and (**F**) right rotation in the lateral lumbar interbody fusion (LLIF), posterior lumbar interbody fusion (PLIF), and transforaminal lumbar interbody fusion (TLIF).

Table 4. The Peak von Mises Stress of Peri-Screw Vertebral Bodies (Unit: MPa)

	LLIF*	PLIF†	TLIF‡
Extension			
L4 left screw	66.5	71.7	78.0
L4 right screw	55.0	55.7	59.2
L5 left screw	37.2	42.2	37.0
L5 right screw	33.0	35.9	40.5
Flexion			
L4 left screw	17.6	22.6	18.1
L4 right screw	14.0	24.0	18.0
L5 left screw	13.3	26.4	30.6
L5 right screw	11.4	21.3	21.7
Lt bending			
L4 left screw	10.7	14.8	15.1
L4 right screw	9.24	11.4	11.3
L5 left screw	7.31	8.42	13.8
L5 right screw	9.04	17.3	21.8
Rt bending			
L4 left screw	11.8	14.3	15.4
L4 right screw	12.1	14.6	13.6
L5 left screw	10.1	18.8	16.5
L5 right screw	7.59	17.2	21.1
Lt rotation			
L4 left screw	26.1	21.9	50.9
L4 right screw	30.2	36.7	33.9
L5 left screw	35.6	50.1	45.6
L5 right screw	33.2	39.7	43.4
Rt rotation			
L4 left screw	40.5	41.5	48.0
L4 right screw	47.5	51.5	48.6
L5 left screw	41.0	48.7	49.2
L5 right screw	32.2	48.7	55.7

*LLIF, lateral lumbar interbody fusion.
†PLIF, posterior lumbar interbody fusion.
‡TLIF, transforaminal lumbar interbody fusion.

The results demonstrated that the peak of stresses in the posterior implant and peri-screw vertebral bodies was the lowest at LLIF, followed by PLIF and TLIF.

In this study, we examined the validity of the model based on previous studies. The ROM of L3–L4 in extension, flexion, left bending, right bending, left rotation, and right rotation was 2.03°, 4.14°, 4.10°, 3.56°, 1.16°, and 1.34°, respectively, in our study. Niosi et al.[25] reported that the ROM of L3–L4 in extension, flexion, bending, and rotation was 2.4 ± 0.9°, 4.4 ± 2.0°, 2.4 ± 1.2°, and 1.2 ± 0.5, respectively. Schmoelz et al.[21] reported that the ROM of L3–L4 in extension, flexion, bending, and rotation was 5.0 ± 1.0°, 4.0 ± 1.3°, 4.7 ± 2.0°, and 1.0 ± 0.6, respectively. As a result, our study was within the range of previous in vitro studies (Table 2). Additionally, the ROM of L4–L5 in extension, flexion, left bending, right bending, left rotation, and right rotation in our study was 3.23°, 4.25°, 5.01°, 5.45°, 1.01°, and 1.16°, respectively. Schilling et al.[22] reported that the ROM of L4–L5 in extension, flexion, bending, and rotation was 3.32 ± 1.12°, 5.62 ± 2.17°, 7.76 ± 1.85°, and 5.16 ± 1.30°, respectively. Shim et al.[23] reported that the ROM of L4–L5 in extension, flexion, bending, and rotation was 2.79 ± 0.42°, 5.48 ± 0.88°, 4.45 ± 1.01°, and 3.80 ± 0.99, respectively. Consequently, our study was within the range of previous in vitro studies, except for rotation (Table 2). Therefore, for rotation, we compared our results with those of the FE study. Yang et al.[24] reported that the ROM of L4–L5 in left rotation and right rotation was 0.90° and 0.96°, respectively. Accordingly, our study is consistent with that study (Table 2). Hence, our intact L3–L5 FE model was proven to be accurate and could be used for analysis.

The von Mises stress of the posterior implant was lowest in the LLIF in our study. The reason was thought to be that LLIF has the advantage of preserving anatomical structures such as vertebral bodies and ligaments of the posterior lumbar spine[25] as compared to PLIF and TLIF. This may have led to increased stability and lower von Mises stresses in the posterior implant. Stress concentration on the posterior implants causes implant fracture, and lower stresses denote that there are fewer chances that the implant will be fractured. Therefore, our study suggested that LLIF was less likely to cause implant fracture.

In addition, the von Mises stresses on the posterior implant in LLIF were lower, especially in flexion and lateral bending compared to PLIF and TLIF. The reason was thought to be that a larger cage can be inserted since the disc cavity can be widely exposed in LLIF.[3] This allows the LLIF to place the cage on the anterior surface of the intervertebral space and the surrounding edge of the vertebral body. This has the advantage of facilitating the braking of movement during the forward and lateral motions, which increases stability. This may have contributed to the reduction in von Mises stresses in the posterior implant.

In this study, the peak von Mises stress of TLIF (83.6 MPa) in the posterior implant was greater than that of PLIF (66.2 MPa). Fan et al.[5] reported that the peak von Mises stress in the posterior implants in PLIF was 88.7 MPa and that in TLIF was 99.4 MPa. Xu et al.[4] reported that the peak von Mises stress in the pedicle screw was greater in TLIF than that in PLIF. Thus, our study was similar to the previous studies. In other words, TLIF is more likely to cause implant fracture than PLIF. Fan et al.[5] reported that the increased stress on the posterior implant in TLIF may be due to the complete resection of the unilateral facet joint; however, they have not reported the mechanism in detail. The facet joints play a role in stabilizing the spine in flexion and extension and restricting excessive axial rotation.[26-29] Previous prefacetectomy and postfacetectomy studies have shown that the facet joints may support 25% of the axial compressive forces and 40%–65% of the rotational and shear forces on the lumbar spine.[27-29] As such,

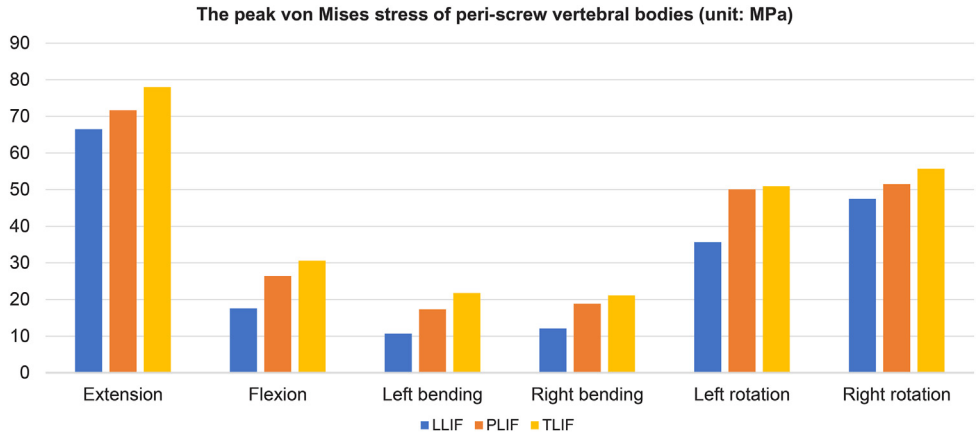

Figure 4. Comparison of the peak von Mises stress of peri-screw vertebral bodies in the lateral lumbar interbody fusion (LLIF), posterior lumbar interbody fusion (PLIF), and transforaminal lumbar interbody fusion (TLIF).

facetectomy may affect lumbar spine stability. In PLIF, depending on the method, the facet joints are often preserved; however, in TLIF, the entire facet joint on one side is removed. Therefore, TLIF, which has a resected unilateral facet joint, is likely to increase instability as compared with PLIF, which has a preserved facet joint. This is a possible factor that may increase von Mises stress in the posterior implant. Although the supraspinous and interspinous ligaments are resected in PLIF, these are structurally

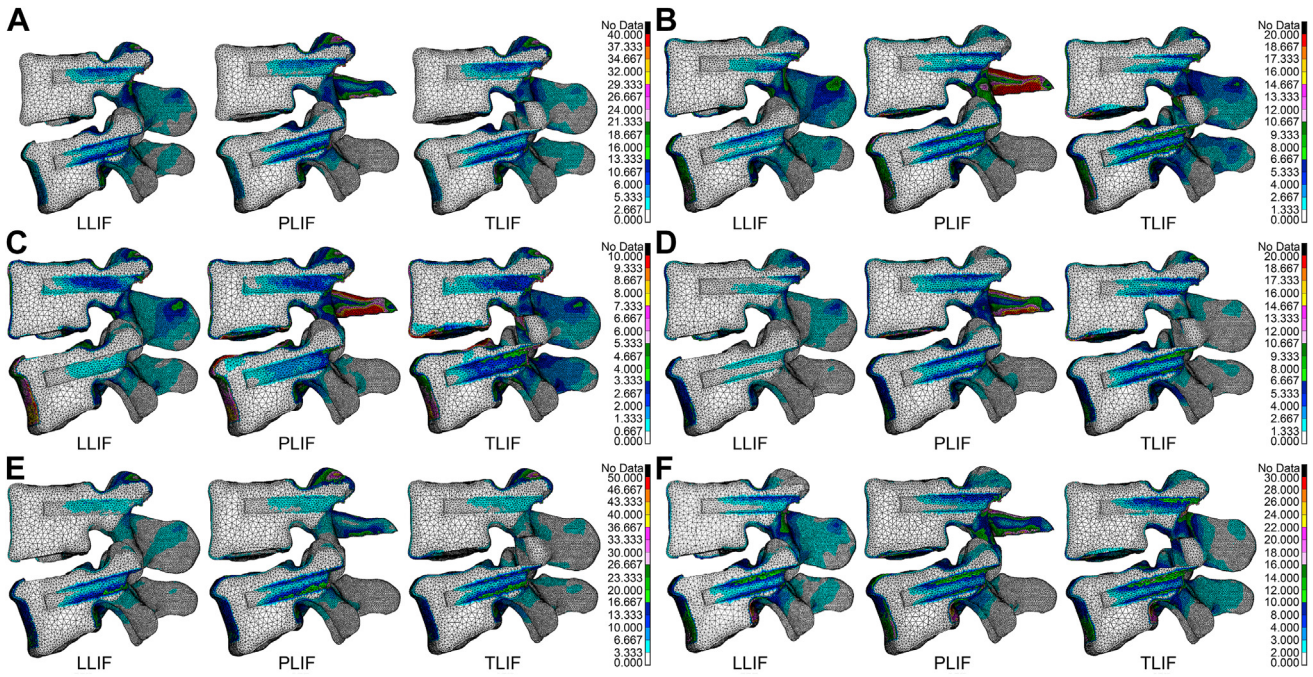

Figure 5. Stress concentration in the peri-screw vertebral bodies. (**A**) Extension, (**B**) flexion, (**C**) left bending, (**D**) right bending, (**E**) left rotation, and (**F**) right rotation in the lateral lumbar interbody fusion (LLIF), posterior lumbar interbody fusion (PLIF), and transforaminal lumbar interbody fusion (TLIF).

weaker ligaments[6] and may not be affected as much as the facet joint resected in TLIF.

We evaluated the stresses in the peri-screw vertebral bodies in the LLIF, PLIF, and TLIF and revealed that it was lowest at LLIF, followed by PLIF and TLIF. Previous studies have reported that an increase in stress in the vertebral body can cause trabecular bone injury and inflammation.[6] In addition, Mueller et al.[30] reported that peri-implant trabecular bone failure caused a fixation failure. However, a few studies have evaluated the stresses on the peri-screw vertebral bodies after spinal fusion,[31] and none have evaluated them after lumbar interbody fusion. In this study, by comparing and evaluating the stress on the peri-screw vertebral bodies in lumbar interbody fusion, we thought that we could compare the ease of degeneration of the peri-screw vertebral bodies, which may also cause screw loosening. Therefore, we suggest that screw loosening is least likely to occur in LLIF and most likely to occur in TLIF.

Our study has several limitations. First, muscles were not considered, which may compromise the model's accuracy. Second, we were unable to reproduce the detailed shape of the interbody cage due to the unavailability of a detailed cage design. Third, the CT images of adult females were used to create the model, and it was not possible to reproduce the degenerative changes that are often seen in elderly patients who underwent interbody fusion surgery. Fourth, we did not take osteoporosis into account when creating the FE model. Fifth, we did not consider the improvement of spinal alignment after lumbar interbody fusion.

Despite these limitations, we were able to analyze the stresses among LLIF, PLIF, and TLIF. It could be predicted that implant failure such as implant fracture and screw loosening was least likely to occur in LLIF, followed by PLIF and TLIF. Hence, surgeons should be aware of these factors when selecting an appropriate surgical technique and be careful for implant failure during postoperative follow-up.

CRediT AUTHORSHIP CONTRIBUTION STATEMENT

Ryo Oikawa: Conceptualization, Data curation, Investigation, Methodology, Visualization, Writing — original draft. **Hideki Murakami:** Conceptualization, Project administration, Supervision, Writing — review & editing. **Hirooki Endo:** Conceptualization, Methodology, Supervision. **Hirotaka Yan:** Conceptualization, Methodology, Resources, Supervision, Writing — review & editing. **Daisuke Yamabe:** Supervision. **Yusuke Chiba:** Supervision. **Ryosuke Oikawa:** Supervision. **Norihiro Nishida:** Methodology, Resources, Supervision, Writing — review & editing. **Xian Chen:** Methodology, Resources. **Takashi Sakai:** Supervision. **Minoru Doita:** Supervision.

REFERENCES

1. Vos T, Flaxman AD, Naghavi M, et al. Years lived with disability (YLDs) for 1160 sequelae of 289 diseases and injuries 1990-2010: a systematic analysis for the Global Burden of Disease Study 2010. *Lancet*. 2012;380:2163-2196.

2. Hill JC, Konstantinous K, Egbewale BE, Dunn KM, Lewis M, van der Windt D. Clinical outcomes among low back pain consulters with referred leg pain in primary care. *Spine (Phila Pa 1976)*. 2011;36:2168-2175.

3. Xu DS, Walker CT, Godzik J, Turner JD, Smith W, Uribe JS. Minimally invasive anterior, lateral, and oblique lumbar interbody fusion: literature review. *Ann Transl Med*. 2018;6:104.

4. Xu H, Tang H, Guan X, et al. Biomechanical comparison of posterior lumbar interbody fusion and transforaminal lumbar interbody fusion by finite element analysis. *Neurosurgery*. 2013;72(Suppl Operative):21-26.

5. Fan W, Guo LX. A comparison of the influence of three different lumbar interbody fusion approaches on stress in the pedicle screw fixation system: finite element static and vibration analyses. *Int J Numer Method Biomed Eng*. 2019;35:e3162.

6. Chepurin D, Chamoli U, Diwan AD. Bony stress and its association with intervertebral disc generation in the lumbar spine: a systematic review of clinical and basic science studies. *Glob Spine J*. 2021, 21925682211008837.

7. Erbulut DU. Biomechanical effect of graded facetectomy on asymmetrical finite element model of the lumbar spine. *Turk Neurosurg*. 2014;24:923-928.

8. Lu T, Lu Y. Comparison of biomechanical performance among posterolateral fusion and transforaminal, extreme, and oblique lumbar interbody fusion: a finite element analysis. *World Neurosurg*. 2019;129:e890-e899.

9. Xu H, Ju W, Xu N, et al. Biomechanical comparison of transforaminal lumbar interbody fusion with 1 or 2 cages by finite element analysis. *Neurosurgery*. 2013;73(Suppl Operative): ons198-ons205 [discussion: ons205].

10. Shirazi-Adl A, Ahmed AM, Shrivastava SC. Mechanical response of a lumbar motion segment in axial torque alone and combined with compression. *Spine (Phila Pa 1976)*. 1986;11:914-927.

11. Zhong ZC, Wei SH, Wang JP, Feng CK, Chen CS, Yu CH. Finite element analysis of the lumbar spine with a new cage using a topology optimization method. *Med Eng Phys*. 2006;28:90-98.

12. Dreischarf M, Zander T, Shirazi-Adl A, et al. Comparison of eight published static finite element models of the intact lumbar spine: predictive power of models improves when combined together. *J Biomech*. 2014;47:1757-1766.

13. Ayturk UM, Puttlitz CM. Parametric convergence sensitivity and validation of a finite element model of the human lumbar spine. *Comput Methods Biomech Biomed Engin*. 2011;14:695-705.

14. Faizan A, Kiapour A, Kiapour AM, Goel VK. Biomechanical analysis of various footprints of transforaminal lumbar interbody fusion devices. *J Spinal Disord Tech*. 2014;27:E118-E127.

15. Chosa E, Goto K, Totoribe K, Tajima N. Analysis of the effect of lumbar spine fusion on the superior adjacent intervertebral disk in the presence of disk degeneration, using the three-dimensional finite element method. *J Spinal Disord Tech*. 2004;17:134-139.

16. Xiao ZT, Wang LY, Gong H, Zhu D. Biomechanical evaluation of three surgical scenarios of posterior lumbar interbody fusion by finite element analysis. *Biomed Eng Online*. 2012;11:31.

17. Vadapalli S, Sairyo K, Goel VK, et al. Biomechanical rationale for using polyetheretherketone (PEEK) spacers for lumbar interbody fusion-A finite element study. *Spine (Phila Pa 1976)*. 2006;31:E992-E998.

18. Imai K. Computed tomography-based finite element analysis to assess fracture risk and osteoporosis treatment. *World J Exp Med*. 2015;5:182-187.

19. Brekelmans WA, Poort HW, Slooff TJ. A new method to analyse the mechanical behaviour of skeletal parts. *Acta Orthop Scand*. 1972;43:301-317.

20. Niosi CA, Zhu QA, Wilson DC, Keynan O, Wilson DR, Oxland TR. Biomechanical characterization of the three-dimensional kinematic behaviour of the Dynesys dynamic stabilization system: an in vitro study. *Eur Spine J*. 2006;15:913-922.

21. Schmoelz W, Huber JF, Nydegger T, Dipl-Ing, Claes L, Wilke HJ. Dynamic stabilization of the lumbar spine and its effects on adjacent segments: an in vitro experiment. *J Spinal Disord Tech*. 2003;16:418-423.

22. Schilling C, Krüger S, Grupp TM, Duda GN, Blömer W, Rohlmann A. The effect of design parameters of dynamic pedicle screw systems on kinematics and load bearing: an in vitro study. *Eur Spine J*. 2011;20:297-307.

23. Shim CS, Park SW, Lee SH, Lim TJ, Chun K, Kim DH. Biomechanical evaluation of an interspinous stabilizing device, Locker. *Spine (Phila Pa 1976)*. 2008;33:E820-E827.

24. Yang M, Sun G, Guo S, et al. The biomechanical study of extraforaminal lumbar interbody fusion: a three-dimensional finite-element analysis. *J Healthc Eng*. 2017;2017:9365068.

25. Song C, Chang H, Zhang D, Zhang Y, Shi M, Meng X. Biomechanical Evaluation of oblique lumbar interbody fusion with various fixation options: a finite element analysis. *Orthop Surg*. 2021;13:517-529.

26. Inoue N, Orías AAE, Segami K. Biomechanics of the lumbar facet joint. *Spine Surg Relat Res*. 2020;4:1-7.

27. Abumi K, Panjabi MM, Kramer KM, Duranceau J, Oxland T, Crisco JJ. Biomechanical evaluation of lumbar spinal Stability after graded facetectomy. *Spine (Phila Pa 1976)*. 1990;15:1142-1147.

28. Zeng ZL, Zhu R, Wu YC, et al. Effect of graded facetectomy on lumbar biomechanics. *J Healthc Eng*. 2017;2017:7981513.

29. Cohen SP, Raja SN. Pathogenesis, diagnosis, and treatment of lumbar zygapophysial (facet) joint pain. *Anesthesiology*. 2007;106:591-614.

30. Mueller TL, Basler SE, Müller R, van Lenthe GH. Time-lapsed imaging of implant fixation failure in human femoral heads. *Med Eng Phys*. 2013;35:636-643.

31. Sensale M, Vendeuvre T, Schilling C, Grupp T, Rochette M, Dall'Ara E. Patient-specific finite element models of posterior pedicle screw fixation: effect of screw's size and geometry. *Front Bioeng Biotechnol*. 2021;9:643154.

Conflict of interest statement: The authors declare that the article content was composed in the absence of any commercial or financial relationships that could be construed as a potential conflict of interest.

Received 23 February 2022; accepted 13 May 2022

Citation: World Neurosurg. (2022) 164:e835-e843.
https://doi.org/10.1016/j.wneu.2022.05.056

Journal homepage: ***www.journals.elsevier.com/world-neurosurgery***

Available online: ***www.sciencedirect.com***